Abstract 208 PB088

Regulation of oncogenic transcription and tumor growth in pediatric cancers by the CDK9 inhibitor KB-0742

Douglas C. Saffran¹, Evon Poon², Glorymar Ibanez³, Jonathan Nakashima⁴, Suha Naffar-Abu Amara¹, Christina Noe¹, Tressa R. Hood¹, Stephanie LaHaye⁵, Ming-Ju Tsai¹, Sara Heuss² Jonathan Ball⁵, Nikolaus D. Obholzer¹, Pavan Kumar¹, Jorge F. DiMartino¹, Filemon Dela Cruz³, Louis Chesler², Charles Y. Lin¹

¹Kronos Bio, Inc., San Mateo, CA, USA; ²Division of Clinical Studies, The Institute of Cancer Research, London, UK; ³Department of Pediatrics, Memorial Sloan Kettering Cancer Center, New York, NY, USA; ⁴Certis Oncology Solutions, San Diego, CA, USA, ⁵Tempus Labs, Chicago, IL, USA

Background

Disruption of transcriptional regulatory networks that drive normal cellular differentiation and development can result in oncogenic transformation and transcriptional addiction. Many pediatric sarcomas are defined by/harbor oncogenic fusion proteins, resulting from chromosomal translocations such as the *EWSR1* gene fused to an ETS family transcription factor (TF) gene (FLI1 or ERG) in Ewing sarcoma, or PAX3/PAX7 and FOXO1 translocations in alveolar rhabdomyosarcoma. In neuroblastoma, MYCN, a member of the MYC family of TFs, is often amplified and localizes to super enhancer regions, where it rewires lineage-specific transcriptional programs driving oncogenesis.

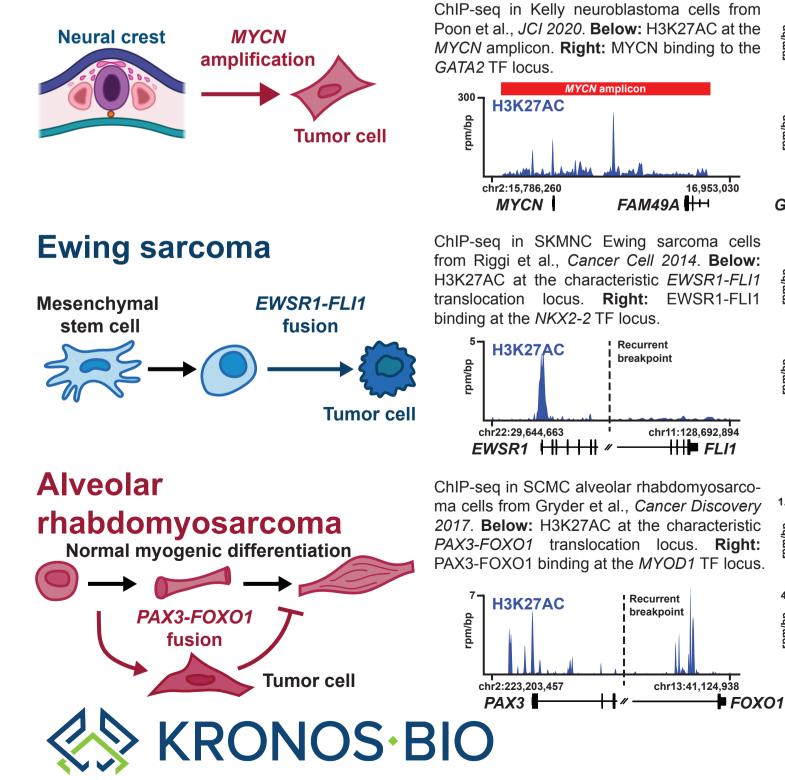
Oncogenic TFs have proven difficult to target directly; we and others have proposed targeting associated transcriptional co-regulators to inhibit their activity. CDK9 interacts with many oncogenic TFs and is essential for TF-mediated transcription elongation through phosphorylation of the C-terminal domain of RNA pol II. KB-0742 is a potent, selective, and orally bioavailable inhibitor of CDK9 currently in clinical development that shows antitumor activity in preclinical models of sarcoma and neuroblastoma.

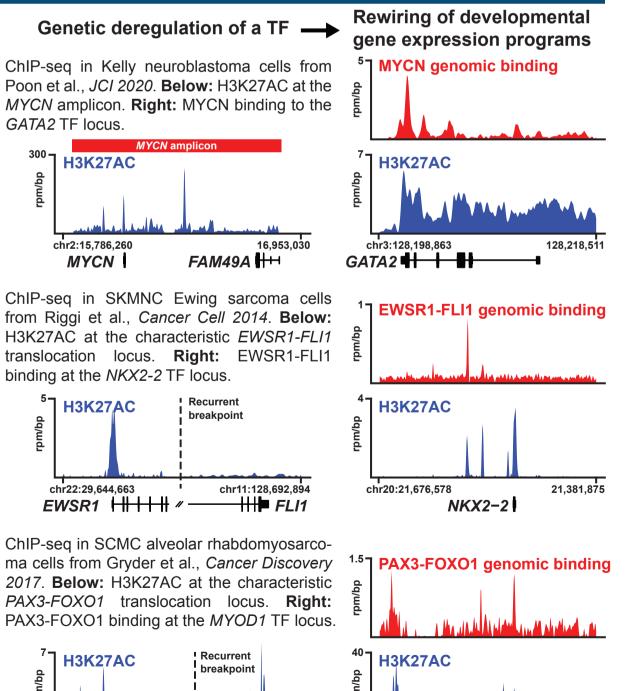
Materials and methods

Cell lines and low-passage patient-derived cells (PDCs) were tested for antiproliferative effects of KB-0742, using either Cell Titer Glo (Promega) or Alamar Blue cell viability reagent (Bio-Rad). Pharmacodynamic (PD) markers of KB-0742 treatment, including phospho-SER2 (pSER2) on RNA pol II, MYCN, MYC, and cleaved poly ADP ribose polymerase (PARP), were measured by Western blot. The antitumor activity of KB-0742 was evaluated using patient-derived xenograft (PDX) models of Ewing sarcoma and alveolar rhabdomyosarcoma in vivo. Tumor samples and plasma were collected to determine PD effects and drug concentrations, respectively. The transgenic TH-MYCN model of neuroblastoma was used to study antitumor effects of KB-0742. All in vivo models were performed according to IACUC guidelines.

Disrupted transcription regulatory networks in pediatric cancers

Neuroblastoma





chr11:17.667.181

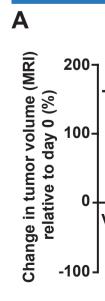
KB-0742 (µM)

0.5

PARF Cleaved PARF

MYC GAPDH

Figure legend: A.B) KB-0742 effects on cell viability across MYCN-amplified or non amplified neuroblastoma cell lines (n=4 each) plated for 24hrs and then treated with KB-0742. A) Continuous treatment. B) 8hr treatment followed by washout. Cell viability measured as surviving fraction of cells 72hrs post treatment. Gl_{eo} concentrations shown as dot plots next to each graph. Differences between groups assessed by a two-tailed t-test. Blue: non amplified lines. Red: MYCN-amplified lines. C) Western blots were performed on MYCN-amplified (Kelly and BE-2C) and non amplified (SKNAS) neuroblastoma cells at 8hr post treatment with measurement of protein levels for biomarkers of CDK9 inhibition (pSER2), induction of apoptosis (full length and cleaved PARP) and MYCN or MYC. GAPDH is provided as a negative control. D) Densitometry of MYCN or MYC protein levels from figure C) normalized to GAPDH with untreated (0µM) levels set to 100%.



17 754 44

MYOD1

Overall results

KB-0742 decreased the viability of immortalized and low passage PDCs from Ewing sarcoma, alveolar rhabdomyosarcoma, and neuroblastoma. In neuroblastoma, cell lines with MYCN amplification were more sensitive to KB-0742 treatment. KB-0742-treated neuroblastoma cells had decreased pSER2, loss of expression of MYCN and MYC, and an induction of cleaved PARP. KB-0742 treatment of a TH-MYCN transgenic mouse model resulted in regression of established tumors. In PDX models of Ewing sarcoma and alveolar rhabdomyosarcoma, KB-0742 treatment inhibited tumor growth. Analysis of tumor samples revealed decreases in pSER2 and the expression of oncogenic fusion TFs KB-0742 is being evaluated in a phase I dose-escalation trial in patients with relapsed or refractory solid tumors or Non-Hodgkin's lymphoma (NCT04718675).

KB-0742 inhibits growth of MYCN-amplified neuroblastoma В 8hr treatment followed by washout and Continuous treatment for 72hr Neuroblastoma measurement at 72hr cell lines - SH-EP SKNSH - SKNAS SH-SY5Y CHC-212 p<0.05 - Kellv - BE-2C IMR-10 Non MYCN 0.1 10 Non MYCN 0.1 KB-0742 (µM) amp amp amp amp KB-0742 (µM) MYCN/MYC levels after 8hr KB-0742 treatment SKNAS BE-2C Kellv 0 2.5 5 10 0 2.5 5 10 0 2.5 5 10 pSER2 KB-0742 (µM) 0 2.5 5 10 0 2.5 5 10 0 2.5 5

KB-0742 causes tumor regression in **MYCN-driven** neuroblastoma genetically engineered mouse model

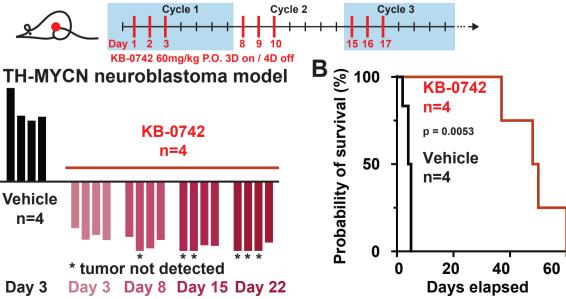


Figure legend: A) The TH-MYCN genetically engineered mouse model was used to assess KB-0742 efficacy in a MYCN-driven model of neuroblastoma. In this model, MYCN is expressed from the tyrosine hydroxylase promoter. Mice which developed evident tumors were either treated with vehicle (saline, n=3) or 60mg/kg KB-0742 (n=4) on a schedule of 3-days on/4-days off per weekly cycle. Tumor volume was assessed by MRI at days 3, 8, 15 and 22. B) Kaplan-Meier plot showing overall survival of vehicle or KB-0742 treated cohorts. Statistical significance of the difference between cohorts is assessed using a log-rank Mantel-Cox test.

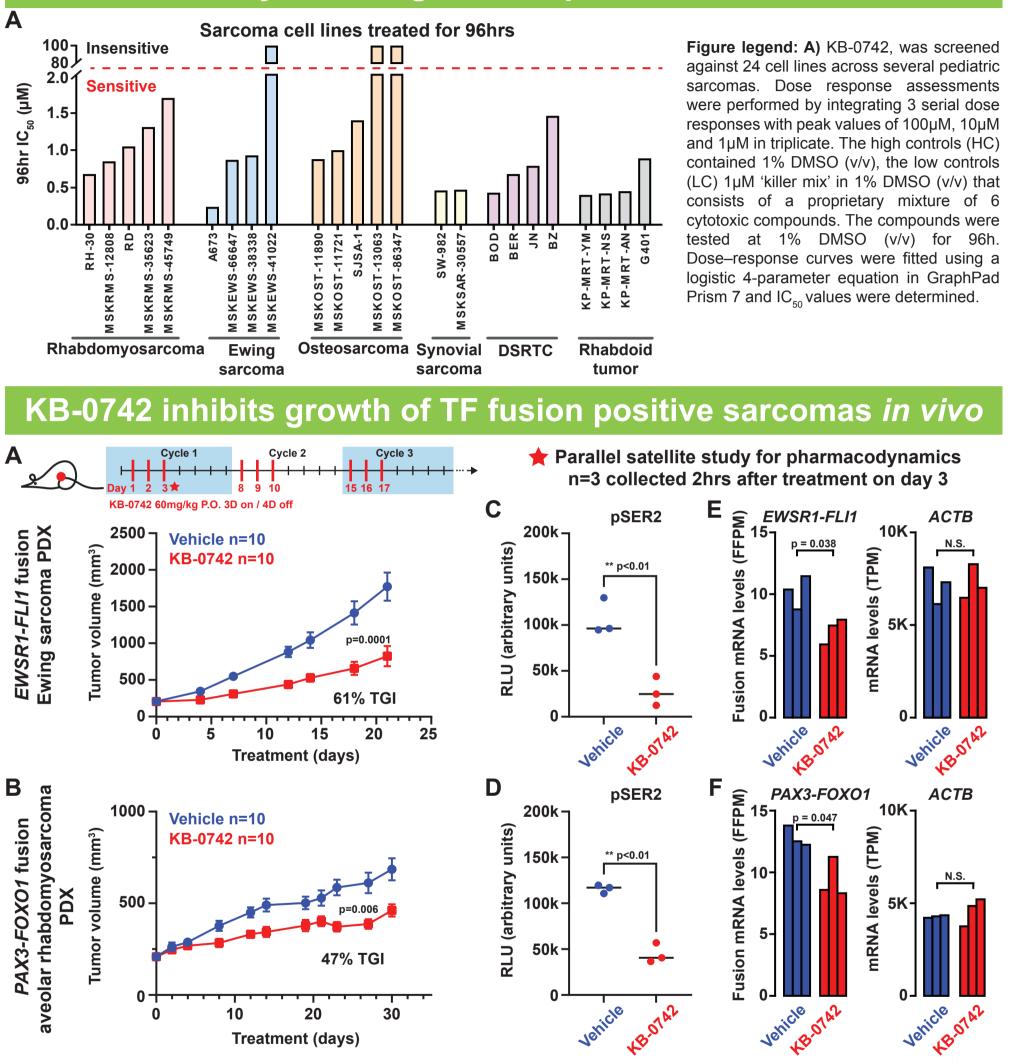


Figure legend: A,B) For PDXs, tumors were subcutaneously engrafted and mice were randomized (n=10 per cohort) at >150mm³ tumo volume. PDX models were treated with vehicle (saline) or 60mg/kg KB-0742 on a 3-days on/4-days off weekly cycle. Tumor volumes and body weights were recorded twice weekly. The statistical difference of growth inhibition between cohorts was denoted and assessed using an unpaired t-test with Welch's correction. C-F) A satellite study was conducted in parallel with tumors (n=3) collected 2hrs post treatment on day 3 in which plasma KB-0742 concentrations of 4µM and 2.5µM were measured in the Ewing sarcoma and aveolar rhabdomyosacroma PDXs respectively. C,D) Tumor lysates were prepared and RNA pol II pSER2 was measured using a Meso Scale Discovery (MSD) assay. Differences in pSER2 levels assessed using two-tailed t-test. E,F) Whole-transcriptome profiling using the Tempus xT assay. Left) RNA fusions detected using STAR-Fusion and Mojo and fusion TF mRNA levels are shown as fusion fragments per million reads (FFPM). Right) An unaffected control mRNA ACTB is shown in units of transcripts per million (TPM). Differences in mRNA levels assessed using two-tailed t-test.

The authors would like to thank Giovanni Rivera, Bianca Carapia, Deborah Yan, Javier Rodriguez, Rowan Prendergast, and Jantzen Sperry from Certis Oncology for their contributions

KB-0742 broadly inhibits growth of pediatric sarcoma cell lines

Acknowledgments